Journal Name

ARTICLE TYPE

Cite this: DOI: 00.0000/xxxxxxxxxx

Supplementary Material†

Superspace approach helps: Determination of proton dynamics in the phase transition of supramolecular ferroelectrics: 5,5'-dimethyl-2,2'-bipyridine and bromanilic acid.

Leila Noohinejad,*[a] Sander van Smaalen,[b] Carsten Paulmann,[a,c] and Martin Tolkiehn[a]

S1 Single-crystal X-ray diffraction.

Diffraction measurements of the four phases could be achieved by special cooling-heating rates employed in the range of 100–360 K. Crystals are radiation and temperature sensitive. Therefore, the complete diffraction experiment involved four different crystals. The cooling/heating profiles were as follows:

1. The first crystal was heated from 298 to 320 K with a rate of 15 K/h and followed by a data collection at 320 K.
2. The second crystal was heated from 298 to 346 K with a rate of 15 K/h, followed by a data collection at 346 K, and finally followed by heating from 346 to 360 K with 15 K/h.
3. The third crystal was cooled from 298 to 245 K with 40 K/h and followed by a data collection at 245 K.
4. The fourth crystal was cooled from 298 to 120 K with 120 K/h and followed by a data collection at 120 K.

Notice that a cooling rate of 120 K/hour is still a small rate, taking 89 minutes to cool from room temperature to 120 K. Furthermore, notice that data collections take several hours.

S2 Crystallographic data of the phases PE-II and FE-I described within the twofold supercell.

Table S1 gives the basic crystallographic information for the ferroelectric phase FE-I and the paraelectric phase PE-II. Both FE-I and PE-II possess twofold superstructures of the high-temperature phase PE-III.

Table S1 Crystallographic data of the phases PE-II and FE-I described within twofold supercell. Refinement is based on only two parameters, scale factor and extinction parameter.

Phase	FE-I	PE-II
Temperature (K)	120	245
Space group	$P1$	$P\bar{1}$
a (Å)	8.783(1)	8.85517(12)
b (Å)	9.753(1)	9.75500(10)
c (Å)	11.8506(3)	12.0004(3)
α (°)	97.1059(24)	96.820(2)
β (°)	104.5443(22)	105.546(2)
γ (°)	115.867(2)	114.739(2)
V (Å^3)	851.9(9)	874.89(4)
nr. Reflections (obs, all)	14212, 14821	5571, 8249
GOF^{obs}, GOF^{all}	6.61, 6.48	4.02, 3.24
R_F^{obs}, R_F^{all} (all)	0.041, 0.0455	0.0390, 0.0450
$\Delta\rho_{max}$, $\Delta\rho_{min}$ (e Å^{-3})	1.65, -1.44	0.58 , -0.48

*E-mail: leila.noohinejad@desy.de ‡E-mail: smash@uni-bayreuth.de.
[a] P24, Photon Science, Deutsches Elektronen-Synchrotron (DESY), D-22607 Hamburg, Germany.
[b] Laboratory of Crystallography, University of Bayreuth, D-95440 Bayreuth, Germany.
[c] Mineralogisch-Petrographisches Institute, University of Hamburg, D-20146 Hamburg, Germany

S3 Torsion angles about C9–C9′ of 55DMBP

Table S2 gives the three bending angles around torsion bond (C9–C9*). for simplicity we call them angles A, B, and C, (see Fig. 9 in main manuscript).Angle A shows the largest change upon transition from FE-I phase to the high-temperature phase PE-III. At PE-IC phase A, B and C angles exhibit large variations in dependence on the phase t of the modulation (Fig. S2).

Table S2 Selected bond angles (deg) so called bending angles, i.e. A, B and C (see Fig. 9) around the torsion bond C9–C9^{i} at PE-IC and PE-III phases and the corresponding bond C9-1(b)–C9-2(b) at FE-I, PE-II phases. (max-min) provides the difference between maximum (max) and minimum (min) separation in dependence on the phase t of the modulation in the PE-IC phase. Mean gives the value averaged over t. Standard uncertainties are given in parentheses.

Bond angle	FE-I	PE-II [a]	PE-IC	max-min	PE-III
A					
C8–C9–C9^{i}			122.345(3) (mean) 121.699(2) (min) 122.900(3) (max)	1.201	123.03(18)
C8-1–C9-1–C9-2	121.491(2)	122.567(2)			
C8-2–C9-2–C9-1	121.899(2)	122.527(2)			
C8-1b–C9-1b–C9-2b	121.511(2)				
C8-2b–C9-2b–C9-1b	122.304(2)				
B					
N1–C9–C9^{i}			117.222(2) (mean) 116.638(2) (min) 117.592(2) (max)	0.954	117.5(3)
N1-1–C9-1–C9-2	116.855(2)	118.105(2)			
N1-2–C9-2–C9-1	116.650(2)	118.137(2)			
N1-1b–C9-1b–C9-2b	117.487(2)				
N1-2b–C9-2b–C9-1b	120.627(3)				
C					
N1–C9–C8			120.347(2) (mean) 119.520(2)(min) 121.537(2)(max)	2.017	119.4(3)
N1-1–C9-1–C8-1	120.639(3)	119.335(2)			
N1-2–C9-2–C8-2	121.127(2)	119.324(2)			
N1-1b–C9-1b–C8-1b	120.838(2)				
N1-2b–C9-2b–C8-2b	121.128(3)				

[i] $-x+1,-y+1,-z+2$.

S4 Crystallographic data of the PE-IC phase at 320 K

For the incommensurately modulated structure of the phase PE-IC at 320 K, the atomic coordinates and modulation parameters are given in Tables S3–S5. Selected geometric parameters are given in Tables S6 and S7. t-Plots of selected geometric parameters are provided in Figures S1 and S2.

Table S3 Fractional atomic coordinates x, y, z and the equivalent isotropic ADP (U_{iso}) of the basic structure, together with the first-order harmonic parameters describing displacive modulation of the incommensurately modulated structure of phase PE-IC. For each atom is given the basic-structure coordinates (first line), sine coefficients of the modulation function (s,1), and cosine coefficients (c,1). Standard uncertainties are given in parentheses.

Atom		x	y	z	U_{iso}
Br1		0.8797	0.1761	0.4405	0.043964
	s,1	-0.0001	-0.0001	0.0002	
	c,1	0.0105	0.0058	-0.0156	
O1		0.715	0.3974	0.2847	0.045073
	s,1	0.0008	-0.0044	0.0023	
	c,1	-0.0019	0.0135	-0.007	
O2		0.5944	0.3438	0.6645	0.045571
	s,1	0.0074	-0.001	-0.0031	
	c,1	0.0222	-0.0028	-0.009	
C7		-0.0003	0.2277	1.0066	0.034009
	s,1	-0.0284	0.0233	0.0035	
	c,1	0.0251	-0.0211	-0.0031	
C8		0.2301	0.3571	1.0537	0.033475
	s,1	0.0128	-0.0105	-0.0011	
	c,1	0.0264	-0.0223	-0.0026	
C5		0.0707	0.2541	0.8176	0.035534
	s,1	0.0223	-0.0178	-0.0043	
	c,1	-0.0112	0.0084	0.002	
C9		0.3754	0.4311	0.9788	0.030973
	s,1	-0.0091	0.0052	0.002	
	c,1	-0.0073	0.0043	0.0016	
N1		0.2906	0.3797	0.8624	0.027774
	s,1	-0.0038	0.0031	0.0007	
	c,1	-0.0395	0.0304	0.0066	
C1		0.6212	0.4403	0.3866	0.034497
	s,1	0.0011	-0.0014	0.0002	
	c,1	-0.0054	0.0071	-0.0015	
C2		0.5548	0.4129	0.5852	0.034517
	s,1	0.0014	-0.0007	-0.0007	
	c,1	0.009	-0.0038	-0.0033	
C3		0.6665	0.3596	0.473	0.032103
	s,1	0	0.0001	0	
	c,1	0.0016	0.0013	-0.0118	
C4		-0.3236	0.0287	0.8284	0.047927
	s,1	-0.003	0.0021	0.0002	
	c,1	-0.0289	0.0214	0.0029	
C6		-0.0829	0.1714	0.8862	0.036923
	s,1	-0.0143	0.0107	0.0007	
	c,1	-0.0012	0.0009	0	
H1		0.6048	0.5442	0.2439	0.06761
	s,1	-0.0253	0.0281	0.0115	
	c,1	0.0934	-0.0693	-0.0268	

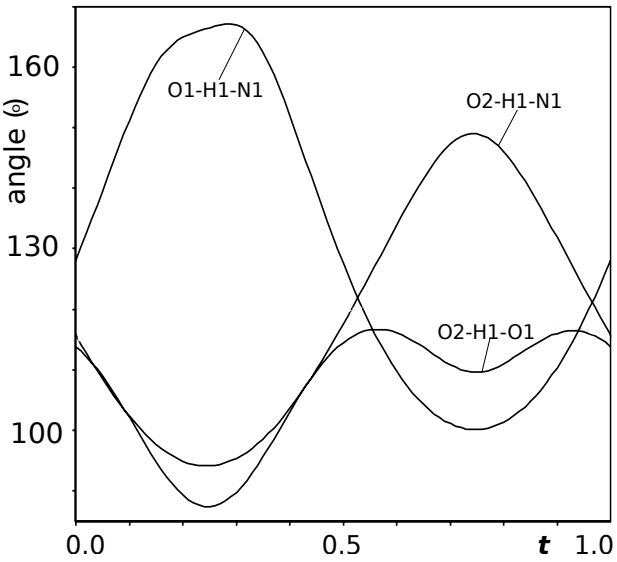

Fig. S1 Hydrogen bond angles (°) in the PE-IC phase as a function of the phase of modulation wave, t.

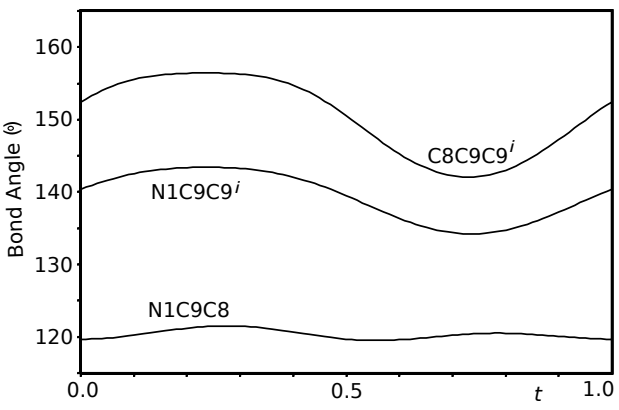

Fig. S2 Bending angles (deg) in 55DMBP as a function of t.

Table S4 Harmonic atomic displacement parameters (ADP) for Br atom of the basic structure, together with the first-order harmonic ADPs describing modulation at 320 K. The basic-structure ADPs (first line), sine coefficients of the modulation function (s,1), and cosine coefficients (c,1). Standard uncertainties are given in parentheses.

Atom		U_{11}	U_{12}	U_{13}	U_{22}	U_{23}	U_{33}
Br1		0.04670(15)	0.04317(15)	0.04438(15)	0.01705(9)	0.00471(8)	0.01318(9)
	s,1	-0.00004(9)	-0.00021(8)	-0.00022(11)	0.00004(7)	0.00009(8)	-0.00011(7)
	c,1	0.00008(9)	-0.00189(7)	0.00895(10)	-0.00080(7)	-0.00307(8)	-0.00331(7)

Table S5 Asymmetric (3rd order) anharmonic ADP parameters for the Br atom at 320 K. Standard uncertainties are given in parentheses.

Atom:	Br1		
C_{111}	-0.0124(7)	C_{133}	-0.00044(6)
C_{112}	-0.0042(2)	C_{222}	-0.00074(17)
C_{113}	0.00001(14)	C_{223}	-0.00020(6)
C_{122}	-0.00133(14)	C_{233}	-0.00041(4)
C_{123}	0.00006(6)	C_{333}	0.00053(5)

Table S6 Bond lengths (Å) with average, minimum and maximum values as determined over the phase t of the modulation wave. Standard uncertainties are given in parentheses

Bond	ave	min	max
Br1-C3	1.8750(3)	1.8731(3)	1.8769(3)
O1-C1	1.25956(8)	1.19465(8)	1.32680(8)
O2-C2	1.255229(15)	1.20211(3)	1.31148(3)
O2-H1^{i}	1.6288(3)	0.7427(5)	2.5374(5)
C7-C8	1.3894(4)	1.3856(5)	1.3924(5)
C7-C6	1.38333(6)	1.37307(9)	1.40257(9)
C8-C9	1.39456(18)	1.3740(3)	1.4175(3)
C8-H8	0.95984(4)	0.95160(7)	0.96825(7)
C5-N1	1.3362(4)	1.3307(5)	1.3407(5)
C5-C6	1.3954(2)	1.3754(3)	1.4158(3)
C9-C9^{ii}	1.4820(5)	1.4813(5)	1.4826(5)
C9-N1	1.34673(6)	1.33536(11)	1.35802(11)
C1-C2^{i}	1.5173(2)	1.5080(2)	1.5281(2)
C1-C3	1.401134(17)	1.33969(2)	1.46663(2)
C2-C3	1.40783(10)	1.34534(12)	1.47437(12)
C4-C6	1.4998(4)	1.4968(5)	1.5034(5)
C7-H7	0.95985(13)	0.95007(18)	0.96986(18)
C8-H8	0.95984(4)	0.95160(7)	0.96825(7)
C4-H6a	0.95998(5)	0.95861(8)	0.96138(8)
C4-H6b	0.95999(16)	0.95929(17)	0.96071(17)
C4-H6c	0.95999(13)	0.95947(14)	0.96050(14)
C5-H5	0.95991(4)	0.95453(6)	0.96536(6)
Symmetry codes:	(i) -x+1,-y+1,-z+1	(ii)-x+1,-y+1,-z+2	

Table S7 Bond angles (deg) with average, minimum and maximum values as determined over the phase t of the modulation wave at 320 K. Standard uncertainties are given in parentheses.

Angle	ave	min	max
C2-O2-H1^{i}	97.323(2)	85.738(2)	115.641(2)
C8-C7-C6	120.548(2)	119.890(2)	121.076(2)
C7-C8-C9	119.193(3)	118.704(2)	119.535(3)
N1-C5-C6	123.322(3)	123.103(3)	123.576(2)
C8-C9-C9^{ii}	122.345(3)	121.699(2)	122.900(3)
C8-C9-N1	120.347(2)	119.520(2)	121.537(2)
C9^{ii}-C9-N1	117.222(2)	116.638(2)	117.592(2)
C5-N1-C9	119.842(2)	118.403(2)	120.767(2)
O1-C1-C2^{i}	117.1376(18)	116.5452(18)	117.8726(18)
O1-C1-C3	123.886(2)	122.685(2)	124.839(2)
C2^{i}-C1-C3	118.969(2)	117.441(2)	120.655(2)
O2-C2-C1^{i}	117.737(2)	117.005(2)	118.601(2)
O2-C2-C3	122.475(2)	121.447(2)	123.204(2)
C1^{i}-C2-C3	119.7863(18)	118.2441(18)	121.5290(18)
Br1-C3-C1	120.100(2)	117.914(2)	122.450(2)
Br1-C3-C2	118.6422(18)	116.4463(18)	121.0052(18)
C1-C3-C2	121.220(2)	120.995(2)	121.510(2)
C7-C6-C5	116.677(2)	115.971(2)	117.365(2)
C7-C6-C4	123.336(2)	122.314(2)	124.141(2)
C5-C6-C4	119.985(3)	119.796(3)	120.320(2)
Symmetry codes:	(i) -x+1,-y+1,-z+1	(ii)-x+1,-y+1,-z+2	

S5 Crystallographic data of the PE-III phase at 346 K

Table S8 Fractional atomic coordinates x, y, z and equivalent isotropic ADPs, U_{iso} of the PE-III phase at 346 K. Standard uncertainties are given in parentheses.

Atom	x	y	z	U_{iso}
Br1	0.87540(15)	0.17727(10)	0.44189(7)	0.0888(7)
O1	0.7104(5)	0.3935(3)	0.28617(16)	0.0801(8)
O2	0.5898(5)	0.3478(3)	0.66572(17)	0.0787(8)
C7	-0.0047(6)	0.2310(3)	1.0063(2)	0.0703(9)
C8	0.2227(6)	0.3608(3)	1.0532(2)	0.0653(8)
C5	0.0789(5)	0.2514(3)	0.8176(2)	0.0668(8)
C9	0.3756(4)	0.4315(2)	0.97864(16)	0.0520(6)
C1	0.6194(5)	0.4378(3)	0.38627(18)	0.0608(7)
C2	0.5538(5)	0.4145(3)	0.58484(19)	0.0603(7)
C3	0.6639(5)	0.3601(3)	0.4746(2)	0.0603(7)
C4	-0.3199(6)	0.0291(4)	0.8290(3)	0.0830(11)
C6	-0.0812(5)	0.1729(3)	0.8861(2)	0.0616(8)
N1	0.2973(11)	0.3775(7)	0.8620(4)	0.0670(7)
H1	0.591(2)	0.424(3)	0.732(3)	0.118002

Table S9 Harmonic atomic displacement parameters (ADPs) of 346 K for Br atom. Standard uncertainties are given in parentheses.

Atom	U_{11}	U_{12}	U_{13}	U_{22}	U_{23}	U_{33}
Br1	0.0888(12)	0.0829(11)	0.0898(11)	0.0261(7)	0.0012(7)	0.0159(7)

Table S10 Asymmetric (3rd order) anharmonic ADP parameters for the Br atom at 346 K. Standard uncertainties are given in parentheses.

Atom:	Br1		
C_{111}	-0.0292(16)	C_{133}	0.00246(15)
C_{112}	-0.0116(6)	C_{222}	-0.0019(4)
C_{113}	0.0008(3))	C_{223}	0.00080(13)
C_{122}	-0.0029(3)	C_{233}	0.00068(9)
C_{123}	-0.00040(13)	C_{333}	-0.00296(14)

Table S11 Symmetric (4th order) anharmonic ADP parameters for the Br atom at 346 K. Standard uncertainties are given in parentheses.

Atom:	Br1		
D_{1111}	0.056(6)	D_{1223}	0.00086(19)
D_{1112}	0.0102(18)	D_{1233}	0.00055(12)
D_{1113}	0.0003(10)	D_{1333}	-0.00017(17)
D_{1122}	0.0082(8)	D_{2222}	0.0040(9)
D_{1123}	0.0011(3)	D_{2223}	0.0002(3)
D_{1133}	0.0027(3)	D_{2233}	0.00100(13)
D_{1222}	0.0054(6)	D_{2333}	0.00041(11)
		D_{3333}	0.00133(18)

Table S12 Bond lengths (Å) at 346 K, PE-III phase. Standard uncertainties are given in parentheses.

Bond		Bond	
Br1-C3	1.883(3)	C5-N1	1.337(5)
O1-C1	1.239(3)	C5-H5	0.96
O2-C2	1.265(4)	C9-C9^{i}	1.484(3)
O2-H1	0.84(2)	C9-N1	1.341(5)
C7-C8	1.387(3)	C1-C2^{ii}	1.528(4)
C7-C6	1.377(3)	C1-C3	1.415(4)
C7-H7	0.96	C2-C3	1.388(3)
C8-C9	1.377(3)	C4-C6	1.504(3)
C8-H8	0.96	C5-C6	1.376(4)

Symmetry codes: (i)-x+1,-y+1,-z+2; (ii)-x+1,-y+1,-z+1

Table S13 Bond angles (°) at 346 K, PE-III phase. Standard uncertainties are given in parentheses.

Bond		Bond	
C8-C7-C6	120.8(3)	O2-C2-C3	123.2(2)
C7-C8-C9	119.7(2)	C1^{ii}-C2-C3	120.1(2)
C6-C5-N1	123.5(3)	Br1-C3-C1	119.40(17)
C8-C9-C9^{i}	123.03(18)	Br1-C3-C2	119.0(2)
C8-C9-N1	119.4(3)	C1-C3-C2	121.6(2)
C9^{i}-C9-N1	117.5(3)	C7-C6-C5	116.2(2)
O1-C1-C2^{ii}	117.4(2)	C7-C6-C4	123.5(3)
O1-C1-C3	124.3(2)	C5-C6-C4	120.3(2)
C2^{ii}-C1-C3	118.25(19)	C5-N1-C9	120.4(4)
O2-C2-C1^{ii}	116.7(2)		

Symmetry codes: (i)-x+1,-y+1,-z+2; (ii)-x+1,-y+1,-z+1

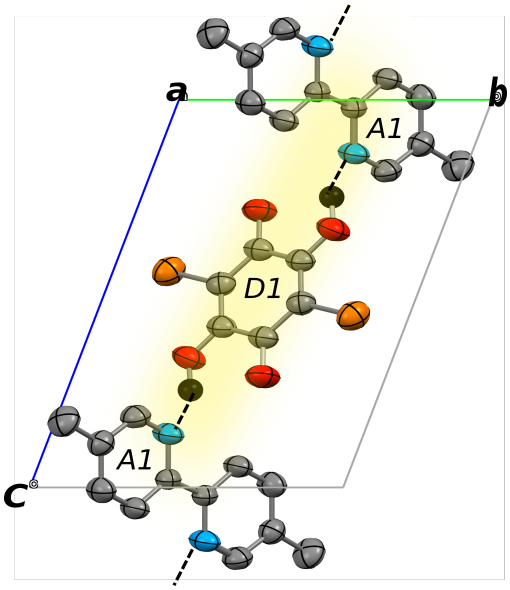

Fig. S3 Projection of the crystal structure of 55DMBP-H_2ba in the PE-III phase at 346 K, viewed along the **a** axis. The space group is $P\bar{1}$. Each molecule is involved in two O—H···N H-bonds (dashed black lines).

S6 *t*-Plots and crystal chemistry for PE-II and FE-I phases

For the PE-II and FE-I phases the effect of proton disorder is demonstrated by *t*-plots. The *t*-plots of O–H and N–H distances relevant for the H-bonds are superimposed for phases FE-I and PE-II in Fig. S4. The *t*-plots of C–C and C–O bond lengths relevant for the observed tautomerism are superimposed for phases Fe-I and PE-II in Fig. S5. These *t* plots can be compared to the *t*-plots of incommensurate FE-IC (Figs. 5 and 6 in the manuscript).

It is to be noticed that all *t* values are relevant for an incommensurate modulation. However, for the presently considered twofold superstructures (commensurate modulation), only two or four *t* values represent distance values realized in the superstructures.

For the phase PE-II with a centrosymmetric superstructure, the two relevant *t*-values are 0.25 and 0.75 (black dashed vertical lines in Figs. S4 and S5).

For the phase FE-I with an acentric twofold superstructure and an optimized *t*-section of $t_0 = 0.72$, the four relevant *t*-values are 0.22, 0.28, 0.72 and 0.78 (blue dashed vertical lines in Figs. S4 and S5).

Employing these *t*-sections, Fig. S4 shows that in phase FE-I, atom H1 is covalently bond to N1 for two out of four H-bonds in the supercell, and it is covalently bonded to O1 for the other two H-bonds. H-bonds are mainly formed with O2 and N1 as acceptor, respectively. In phase PE-II, the H1 atoms are at intermediate positions between the O1 and N1 atoms and slightly farther apart from O2.

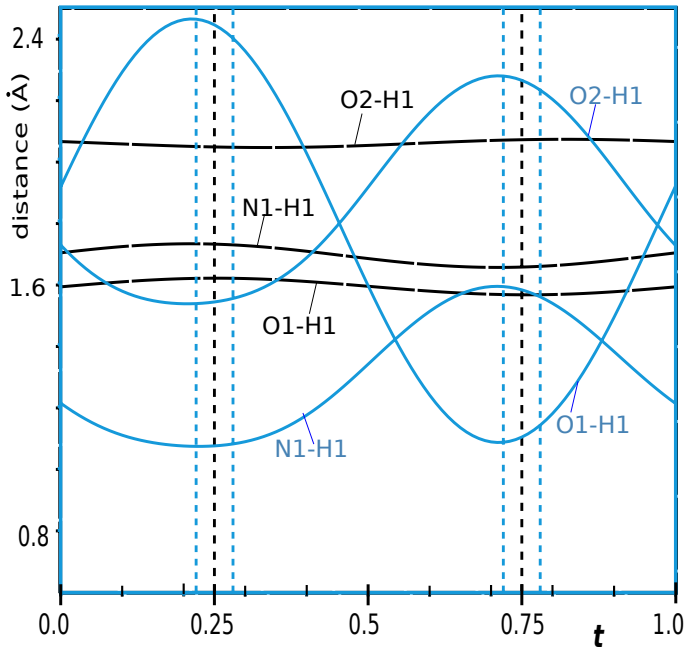

Fig. S4 Geometry of the intermolecular H-bonds represented as *t*-plots for the phase FE-I (thin full blue curves and vertical dashed thin blue lines) and for the phase PE-II (thick long-dashed black curves and vertical dashed thick black lines).

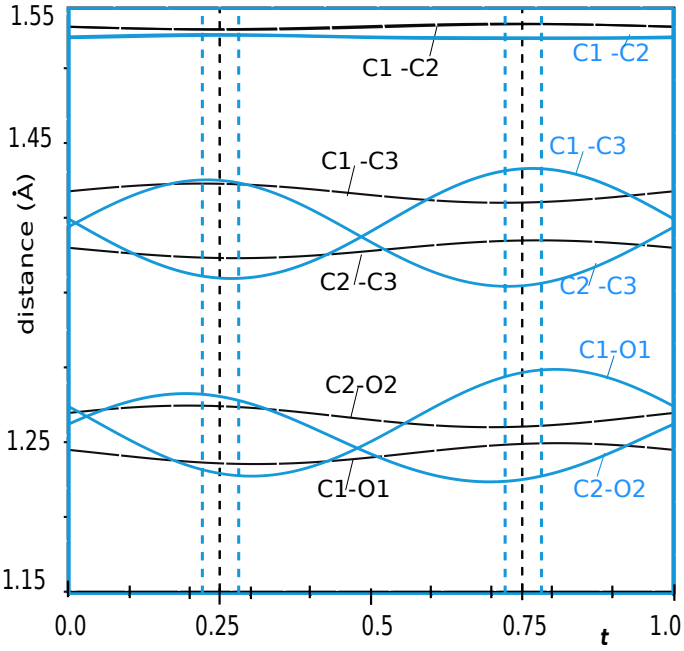

Fig. S5 Selected bond lengths (Å) represented as *t*-plots for the phase FE-I (thin full blue curves and vertical dashed thin blue lines) and for the phase PE-II (thick long-dashed black curves and vertical dashed thick black lines)

S7 Anharmonic displacements of the Br atoms

Introduction of third-order (C_{ijk}) and fourth-order (D_{ijkl}) anharmonic displacement parameters for Br involves an additional 25 parameters. Evidence for anharmonic displacements initially comes from the improved fit to the SXRD data, as signified by a significant drop in R values, as described in Section 2.3. Important evidence for the anharmonic displacements also derives from the resulting structure model. Several parameters C_{ijk} and D_{ijkl} attain values larger than 10 times their standard uncertainties (s.u.). The largest values are C_{111} = -0.0270(16) and D_{1111} = 0.054(6). We believe that a series of parameters larger than 10 times their s.u. is strong evidence for the anharmonic motion of Br. Thirdly, evidence for anharmonic displacements of Br is provided by difference Fourier maps (residual density maps) of sections containing the Br atom. The difference Fourier maps exhibit less structure and smaller maximum and minimum values for a model with anharmonic displacement parameters than for a model without these parameters. See Figs. S6, S7 and S8 for structure models at 245 K, 320 K and 346 K, respectively.

As an alternative model, we have tested a split-atom model for disorder of the Br atom. All attemps to refine such a model resulted in a "singular matrix," thus preventing refinement and providing evidence that the split-atom model does not apply here.

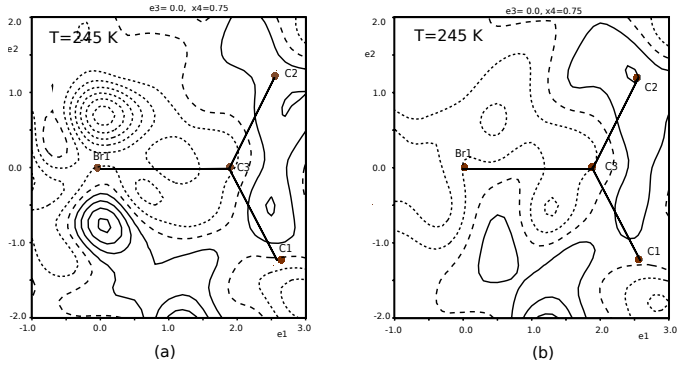

Fig. S6 Section of 4×4 Å^2 of a plane through the atoms Br1, C3 and C2 of the difference Fourier map at T = 245 K, also containing atom C1. This plot is for the commensurate phase PE-II for t-section $t = 0.75$. Positive contours (solid lines), negative contours (dotted lines) and the zero contour (dashed lines) are drawn at intervals of 0.1 electrons/Å^3. Brown dots are the positions of atoms as indicated. (a) Model without anharmonic displacements, and (b) model incorporating anharmonic displacement parameters for Br.

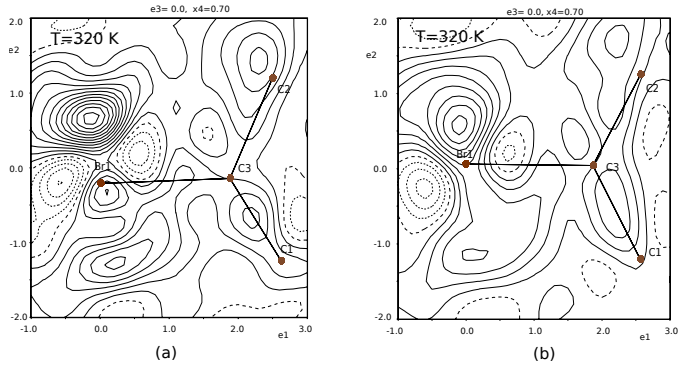

Fig. S7 Section of 4×4 Å^2 of a plane through the atoms Br1, C3 and C2 of the difference Fourier map at T = 320 K, also containing atom C1. This plot is for the incommensurate phase PE-IC for t-section $t = 0.7$. Positive contours (solid lines), negative contours (dotted lines) and the zero contour (dashed lines) are drawn at intervals of 0.1 electrons/Å^3. Brown dots are the positions of atoms as indicated. (a) Model without anharmonic displacements, and (b) model incorporating anharmonic displacement parameters for Br.

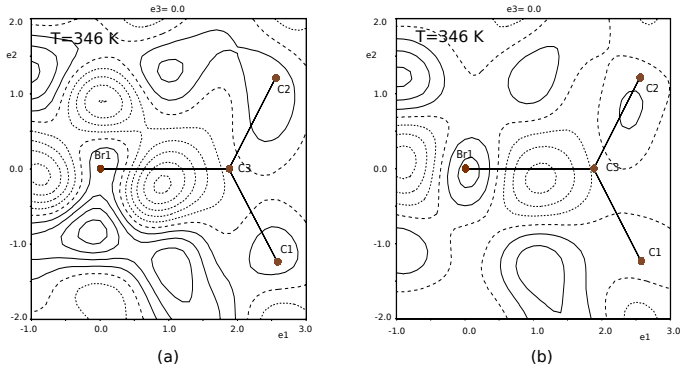

Fig. S8 Section of 4×4 Å^2 of a plane through the atoms Br1, C3 and C2 of the difference Fourier map at T = 346 K, also containing atom C1. Positive contours (solid lines), negative contours (dotted lines) and the zero contour (dashed lines) are drawn at intervals of 0.1 electrons/Å^3. Brown dots are the positions of atoms as indicated. (a) Model without anharmonic displacements, and (b) model incorporating anharmonic displacement parameters for Br.